ANALYSIS OF THERMALLY LOADED LAMINATED CIRCULAR PLATES

Report No. 1

John F. Carney III, Associate Professor

JHRAC Project 70-2 JHR 71-37

April 1971

Abstract

This report summarizes the work done on the two layered phase of the study on thermally loaded laminated circular plates. In this investigation, the roadway system is assumed to be composed of two layers, each with its corresponding modulus of elasticity, Poisson's ratio, and coefficient of thermal expansion. The variation of the modulus of elasticity with depth of pavement is assumed to vary both linearly and parabolically. In addition, two extremes of temperature distribution are considered. In the first case, the temperature distribution is assumed to decrease with depth of pavement, as would be the case at midday. The temperature distribution is then increased with depth to simulate the situation in the early morning hours. The critical stress in the pavement is taken to be the maximum tensile stress.

Based on the results of this phase of the project, the following trends are apparent:

1. The maximum tensile radial stress increases with an increase of Poisson's ratio.
2. The stresses tend to be very sensitive to the ratio of coefficients of thermal expansion of the layers.
3. When $\alpha_1/\alpha_2 \simeq 1$, the individual thicknesses of the layers are not critical parameters if Young's Modulus does not change drastically between the two layers.
4. The parabolic relationship between temperature and Young's Modulus represents a more realistic description of the actual case than does the linear T-E relationship and should be employed unless the temperature range is small.

This work is continuing in the Civil Engineering Department of the University of Connecticut under the sponsorship of the Joint Highway Research Advisory Council of the Connecticut Department of Transportation and the University of Connecticut.

Development of Theory

A two-layered circular plate of radius "a" is considered as shown in Fig. 1. The total displacement of any point in the radial direction, u, and the tangential direction, v, are

$$u = u_o - \frac{\partial w}{\partial r} z \tag{1}$$

and

$$v = v_o - \frac{1}{r} \frac{\partial w}{\partial \theta} z \tag{2}$$

in which u_o and v_o are the displacements at the top surface of the plate in the radial and tangential directions, respectively, while w represents the transverse deflection of the middle plane of the plate.

In polar coordinates, the three strain displacement equations may be expressed as

$$\varepsilon_r = \frac{\partial u}{\partial r} \tag{3}$$

$$\varepsilon_\theta = \frac{u}{r} + \frac{1}{r} \frac{\partial v}{\partial \theta} \tag{4}$$

$$\gamma_{r\theta} = \frac{1}{r} \frac{\partial u}{\partial \theta} + \frac{\partial v}{\partial r} - \frac{v}{r} \tag{5}$$

Substituting Eqs. (1) and (2) into Eqs. (3), (4), and (5) yields

$$\varepsilon_r = \varepsilon_{ro} - \frac{\partial^2 w}{\partial r^2} z \tag{6}$$

$$\varepsilon_\theta = \varepsilon_{\theta o} - \left[\frac{1}{r} \frac{\partial w}{\partial r} + \frac{1}{r^2} \frac{\partial^2 w}{\partial \theta^2} \right] z \tag{7}$$

$$\gamma_{r\theta} = \gamma_{r\theta o} + 2 \left[\frac{1}{r^2} \frac{\partial w}{\partial r} - \frac{1}{r} \frac{\partial^2 w}{\partial r \partial \theta} \right] z \tag{8}$$

In which

$$\varepsilon_{ro} = \frac{\partial u_o}{\partial r} \tag{9}$$

$$\varepsilon_{\theta o} = \frac{u_o}{r} + \frac{1}{r}\frac{\partial v_o}{\partial \theta} \tag{10}$$

and

$$\gamma_{r\theta o} = \frac{1}{r}\frac{\partial u_o}{\partial \theta} - \frac{v_o}{r} + \frac{\partial v_o}{\partial r} \tag{11}$$

In the thermoelastic case, the total strain is the sum of the thermal strain and the stress induced strain. The stress induced strains may be written as

$$\varepsilon_r' = \varepsilon_r - \alpha_i T \tag{12}$$

$$\varepsilon_\theta' = \varepsilon_\theta - \alpha_i T \tag{13}$$

and

$$\gamma_{r\theta}' = \gamma_{r\theta} \tag{14}$$

in which α_i is the coefficient of thermal expansion of the i th layer of the plate, and T is the difference between the actual temperature and the initial, unstressed temperature. In the general case, T is a function of all three coordinates.

The stresses are related to the stress-induced (non-thermal) strains by Hooke's Law as

$$\sigma_{r_i} = \frac{E_i}{1-\nu^2}(\varepsilon_r' + \nu\,\varepsilon_\theta') \tag{15}$$

$$\sigma_{\theta_i} = \frac{E_i}{1-\nu^2}(\varepsilon_\theta' + \nu\,\varepsilon_r') \tag{16}$$

$$\tau_{r\theta_i} = \frac{E_i \gamma_{r\theta}'}{2(1+\nu)} \tag{17}$$

in which E_i is the modulus of elasticity of the i th layer and ν is Poisson's ratio.

Substituting Eqs. (6-14) into Eqs. (15-17) yields

$$\sigma_{r_i} = \frac{E_i}{1-\nu^2}(\varepsilon_{ro} + \nu\,\varepsilon_{\theta o}) - \frac{E_i\alpha_i T}{1-\nu} - \frac{E_i z}{1-\nu^2}\left[\frac{\partial^2 w}{\partial r^2} + \nu\left(\frac{1}{r}\frac{\partial w}{\partial r} + \frac{1}{r^2}\frac{\partial^2 w}{\partial\theta^2}\right)\right] \tag{18}$$

$$\sigma_{\theta_i} = \frac{E_i}{1-\nu^2}(\nu\varepsilon_{ro} + \varepsilon_{\theta o}) - \frac{E_i\alpha_i T}{1-\nu} - \frac{E_i z}{1-\nu^2}\left[\nu\frac{\partial^2 w}{\partial r^2} + \frac{1}{r}\frac{\partial w}{\partial r} + \frac{1}{r^2}\frac{\partial^2 w}{\partial\theta^2}\right] \tag{19}$$

and

$$\tau_{r\theta_i} = \frac{E_i}{2(1+\nu)}\left[\gamma_{r\theta o} + 2z\left(\frac{1}{r^2}\frac{\partial w}{\partial\theta} - \frac{1}{r}\frac{\partial^2 w}{\partial r\partial\theta}\right)\right] \tag{20}$$

At this point, it is convenient to define stress resultants in the form

$$\begin{Bmatrix} N_r \\ N_\theta \\ N_{r\theta} \\ M_r \\ M_\theta \\ M_{r\theta} \end{Bmatrix} = \int_o^h \begin{Bmatrix} \sigma_r \\ \sigma_\theta \\ \tau_{r\theta} \\ \sigma_r z \\ \sigma_\theta z \\ \tau_{r\theta} z \end{Bmatrix} dz \tag{21}$$

in which N_r, N_θ, and $N_{r\theta}$ are forces per unit length while M_r, M_θ, and $M_{r\theta}$ are moments per unit length, and h is the thickness of the plate.

Substituting Eqs. (18-20) into Eq. (21) yields

$$N_r = B(\varepsilon_{ro} + \nu\varepsilon_{\theta o}) - P - C\left[\frac{\partial^2 w}{\partial r^2} + \nu\left(\frac{1}{r}\frac{\partial w}{\partial r} + \frac{1}{r^2}\frac{\partial^2 w}{\partial\theta^2}\right)\right] \tag{22}$$

$$N_\theta = B(\nu\varepsilon_{ro} + \varepsilon_{\theta o}) - P - C\left[\nu\frac{\partial^2 w}{\partial r^2} + \frac{1}{r}\frac{\partial w}{\partial r} + \frac{1}{r^2}\frac{\partial^2 w}{\partial\theta^2}\right] \tag{23}$$

$$N_{r\theta} = B\left(\frac{1-\nu}{2}\right)\gamma_{r\theta o} + C(1-\nu)\left[\frac{1}{r^2}\frac{\partial w}{\partial \theta} - \frac{1}{r}\frac{\partial^2 w}{\partial r \partial \theta}\right] \tag{24}$$

$$M_r = C(\varepsilon_{ro} + \nu\varepsilon_{\theta o}) - Q - D\left[\frac{\partial^2 w}{\partial r^2} + \nu\left(\frac{1}{r}\frac{\partial w}{\partial r} + \frac{1}{r^2}\frac{\partial^2 w}{\partial \theta^2}\right)\right] \tag{25}$$

$$M_\theta = C(\nu\varepsilon_{ro} + \varepsilon_{\theta o}) - Q - D\left[\nu\frac{\partial^2 w}{\partial r^2} + \left(\frac{1}{r}\frac{\partial w}{\partial r} + \frac{1}{r^2}\frac{\partial^2 w}{\partial \theta^2}\right)\right] \tag{26}$$

$$M_{r\theta} = C\left(\frac{1-\nu}{2}\right)\gamma_{r\theta o} + D(1-\nu)\left[\frac{1}{r^2}\frac{\partial w}{\partial \theta} - \frac{1}{r}\frac{\partial^2 w}{\partial r \partial \theta}\right] \tag{27}$$

The quantities B, C, and D in eqs. (22-27) are constants defined respectively as

$$B = \int_o^{t_1} \frac{E_1}{1-\nu^2}\,dz + \int_{t_1}^{t_1+t_2} \frac{E_2}{1-\nu^2}\,dz \tag{28}$$

$$C = \int_o^{t_1} \frac{E_1 z}{1-\nu^2}\,dz + \int_{t_1}^{t_1+t_2} \frac{E_2 z}{1-\nu^2}\,dz \tag{29}$$

$$D = \int_o^{t_1} \frac{E_1 z^2}{1-\nu^2}\,dz + \int_{t_1}^{t_1+t_2} \frac{E_2 z^2}{1-\nu^2}\,dz \tag{30}$$

The quantities P and Q are functions of r and θ and are given by the expressions

$$P = \frac{1}{1-\nu}\left[\int_o^{t_1} \alpha_1 E_1 T\,dz + \int_{t1}^{t_1+t_2} \alpha_2 E_2 T\,dz\right] \tag{31}$$

$$Q = \frac{1}{1-\nu}\left[\int_o^{t_1} \alpha_1 E_1 Tz\,dz + \int_{t_1}^{t_1+t_2} \alpha_2 E_2 Tz\,dz\right] \tag{32}$$

The equilibrium equations in terms of the stress resultants are

$$\frac{\partial N_r}{\partial r} + \frac{1}{r}\frac{\partial N_{r\theta}}{\partial \theta} + \frac{N_r - N_\theta}{r} = 0 \tag{33}$$

$$\frac{\partial N_r}{\partial r} + \frac{1}{r}\frac{\partial N_\theta}{\partial \theta} + \frac{2N_{r\theta}}{r} = 0 \tag{34}$$

$$\frac{\partial Q_r}{\partial r} + \frac{1}{r}\frac{\partial Q_\theta}{\partial \theta} + \frac{Q_r}{r} = 0 \tag{35}$$

$$\frac{\partial M_r}{\partial r} + \frac{1}{r}\frac{\partial M_{r\theta}}{\partial \theta} - Q_r + \frac{M_r - M_\theta}{r} = 0 \tag{36}$$

$$\frac{\partial M_{r\theta}}{\partial r} + \frac{1}{r}\frac{\partial M_\theta}{\partial \theta} - Q_\theta + \frac{2M_{r\theta}}{r} = 0 \tag{37}$$

in which Q_r and Q_θ are transverse shearing forces per unit length. Equations (33) and (34) can be satisfied identically if the Airy Stress Function $F(r,\theta)$ is defined such that

$$N_r = \frac{1}{r}\frac{\partial F}{\partial r} + \frac{1}{r^2}\frac{\partial^2 F}{\partial \theta^2} \tag{38}$$

$$N_\theta = \frac{\partial^2 F}{\partial r^2} \tag{39}$$

$$N_{r\theta} = -\frac{1}{r}\frac{\partial^2 F}{\partial r \partial \theta} + \frac{1}{r^2}\frac{\partial F}{\partial \theta} \tag{40}$$

Substituting Eqs. (36) and (37) into Eq. (35) leads to

$$\frac{\partial^2 M_r}{\partial r^2} + \frac{2}{r}\frac{\partial M_r}{\partial r} - \frac{1}{r}\frac{\partial M_\theta}{\partial r} + \frac{1}{r^2}\frac{\partial M_{r\theta}}{\partial \theta} + \frac{2}{r^2}\frac{\partial M_{r\theta}}{\partial \theta} + \frac{2}{r}\frac{\partial^2 M_{r\theta}}{\partial r \partial \theta} = 0 \tag{41}$$

Substituting Eqs. (22) and (38) into Eq. (25), Eqs. (23) and (39) into Eq. (26), and Eqs. (24) and (40) into Eq. (27) yields, respectively

$$M_r = \frac{C}{B}\left[\frac{1}{r}\frac{\partial F}{\partial r} + \frac{1}{r^2}\frac{\partial^2 F}{\partial \theta^2}\right] + \frac{C}{B}P - Q + \left[\frac{C^2}{B} - D\right]$$

$$\left[\frac{\partial^2 w}{\partial r^2} + \nu\left(\frac{1}{r}\frac{w}{r} + \frac{1}{r^2}\frac{\partial^2 w}{\partial \theta^2}\right)\right] \tag{42}$$

$$M_\theta = \frac{C}{B}P - Q + \left[\frac{C^2}{B} - D\right]\left[\nu\frac{\partial^2 w}{\partial r^2} + \frac{1}{r}\frac{\partial w}{\partial r} + \frac{1}{r^2}\frac{\partial^2 w}{\partial \theta^2}\right] + \frac{C}{B}\frac{\partial^2 F}{\partial r^2} \tag{43}$$

$$M_{r\theta} = \frac{C}{B}\left[\frac{1}{r^2}\frac{\partial F}{\partial \theta} - \frac{1}{r}\frac{\partial^2 F}{\partial r \partial \theta}\right] + (\nu - 1)\left[\frac{C^2}{B} - D\right]$$

$$\left[\frac{1}{r^2}\frac{\partial w}{\partial \theta} - \frac{1}{r}\frac{\partial^2 w}{\partial r \partial \theta}\right] \tag{44}$$

Substituting these expressions for M_r, M_θ, and $M_{r\theta}$ into Eq. (41) results in the first governing differential equation in the form

$$\left[\frac{C^2}{B} - D\right]\nabla^4 w = \nabla^2\left[Q - \frac{C}{B}P\right] \tag{45}$$

in which

$$\nabla^2 = \frac{\partial^2}{\partial r^2} + \frac{1}{r}\frac{\partial}{\partial r} + \frac{1}{r^2}\frac{\partial^2}{\partial \theta^2} \tag{46}$$

and $$\nabla^4 = \nabla^2 \nabla^2 \tag{47}$$

The second governing equation results from the strain capatibility expression for in-plane strains. This expression is obtained from Eqs. (3-5) by eliminating the displacements u and v, and is given by the expression

$$\frac{1}{r^2}\frac{\partial^2\varepsilon_r}{\partial\theta^2} - \frac{1}{r}\frac{\partial\varepsilon_r}{\partial r} + \frac{\partial^2\varepsilon_\theta}{\partial r^2} + \frac{2}{r}\frac{\partial\varepsilon_\theta}{\partial r} - \frac{1}{r}\frac{\partial^2\gamma_{r\theta}}{\partial r\partial\theta} - \frac{1}{r^2}\frac{\partial\gamma_{r\theta}}{\partial\theta} = 0 \qquad (48)$$

Working with Eqs. (22), (23), (24), (38), (39), (40), (6), (7), and (8), yields

$$\varepsilon_r = \frac{1}{B(\nu^2-1)}\left[\nu\frac{\partial^2 F}{\partial r^2} - \left(\frac{1}{r}\frac{\partial F}{\partial r} + \frac{1}{r^2}\frac{\partial^2 F}{\partial\theta^2}\right)\right] + \frac{P}{B(\nu+1)} + \left[\frac{C}{B} - z\right]\frac{\partial^2 w}{\partial r^2} \qquad (49)$$

$$\varepsilon_\theta = \frac{1}{B(\nu^2-1)}\left[\nu\left(\frac{1}{r}\frac{\partial F}{\partial r} + \frac{1}{r^2}\frac{\partial^2 F}{\partial\theta^2}\right) - \frac{\partial^2 F}{\partial r^2}\right] + \frac{P}{B(\nu+1)} + \left[\frac{C}{B} - z\right]\left[\frac{1}{r}\frac{\partial w}{\partial r} + \frac{1}{r^2}\frac{\partial^2 w}{\partial\theta^2}\right] \qquad (50)$$

$$\gamma_{r\theta} = \frac{2}{B(1-\nu)}\left[\frac{1}{r^2}\frac{\partial F}{\partial\theta} - \frac{1}{r}\frac{\partial^2 F}{\partial r\partial\theta}\right] - 2\left[\frac{C}{B} - z\right]\left[\frac{1}{r^2}\frac{\partial w}{\partial\theta} - \frac{1}{r}\frac{\partial^2 w}{\partial r\partial\theta}\right] \qquad (51)$$

These expressions for ε_r, ε_θ, and $\gamma_{r\theta}$ are then substituted into Eq. (48) resulting in the second governing differential equation of the system, written in the form

$$\nabla^4 F = (\nu-1)\,\nabla^2 P \qquad (52)$$

It is interesting to note that the two governing equations given by Eqs. (45) and (52) are uncoupled, even though each was derived from expressions containing both w and F.

As the governing differential equations are of the same general form, their homogeneous solutions will be similar. The general solutions of

Eqs. (45) and (52) may be written as[1]

$$w = w_p + (A_o + B_o r^2 + C_o \ln r + D_o r^2 \ln r)$$
$$+ (A_1 r + B_1 r^3 + C_1 r^{-1} + D_1 r \ln r) \cos\theta$$
$$+ \sum_{n=2}^{\infty} (A_n r^n + B_n r^{-n} + C_n r^{n+2} + D_n r^{-n+2}) \cos n\theta$$
$$+ (A_1' r + B_1' r^3 + C_1' r^{-1} + D_1' r \ln r) \sin\theta$$
$$+ \sum_{n=2}^{\infty} (A_n' r^n + B_n' r^{-n} + C_n' r^{n+2} + D_n' r^{-n+2}) \sin n\theta \qquad (53)$$

$$F = F_p + (G_o + H_o r^2 + I_o \ln r + J_o r^2 \ln r)$$
$$+ (G_1 r + H_1 r^3 + I_1 r^{-1} + J_1 r \ln r) \cos\theta$$
$$+ \sum_{n=2}^{\infty} (G_n r^n + H_n r^{-n} + I_n r^{n+2} + J_n r^{-n+2}) \cos n\theta$$
$$+ (G_1' r + H_1' r^3 + I_1' r^{-1} + J_1' r \ln r) \sin\theta$$
$$+ \sum_{n=2}^{\infty} (G_n' r^n + H_n' r^{-h} + I_n' r^{n+2} + J_n' r^{-n+2}) \sin n\theta \qquad (54)$$

in which w_p and F_p are particular solutions whose forms depend on the character of the right hand sides of Eqs. (45) and (52).

Temperature Distribution and Boundary Conditions

No restrictions have as yet been imposed on the form of the temperature distribution. It may in general be a function of r, θ, and z. For the general case, it will be necessary to expand the right hand sides of Eqs. (45) and (54) in a double Fourier series, significantly complicating the problem. In applying this theory to highway pavements, it is clear

that the majority of realistic temperature distributions will vary only with depth and not with r or θ. In this report, only temperature distributions which vary with depth alone will be considered.

Boundary conditions must be imposed on w, F, and their derivatives. In an attempt to simulate the situation which may exist in a highway pavement, the following boundary conditions will be applied at r = a:

$$(w)_{r=a} = 0 \tag{55}$$

$$\left(\frac{\partial w}{\partial r}\right)_{r=a} = 0 \tag{56}$$

$$(F)_{r=a} = 0 \tag{57}$$

$$\left(\frac{\partial F}{\partial r}\right)_{r=a} = 0 \tag{58}$$

Evaluation of w and F

Since the temperature distibution is a function of depth only, it is seen from Eqs. (31) and (32) that P and Q are constants. Eqs. (45) and (52) are therefore homogeneous and

$$w_p = F_p = 0 \tag{59}$$

Furthermore, the boundary conditions are independent of θ. Therefore, Eqs. (53) and (54) simplify to, respectively,

$$w = A_o + B_o r^2 + C_o \ln r + D_o r^2 \ln r \tag{60}$$

and

$$F = G_o + H_o r^2 + I_o \ln r + J_o r^2 \ln r \tag{61}$$

Applying Eq. (55) to Eq. (60) yields

$$A_o = 0 \tag{62}$$

The fact that the deflection and stress resultants must remain finite at r = 0 leads to

$$C_o = D_o = 0 \tag{63}$$

Finally, applying Eq. (56) to Eq. (60) yields

$$B_o = 0 \tag{64}$$

Therefore,

$$w = 0 \tag{65}$$

Carrying out a similar procedure with respect to Eq. (61) leads to

$$F = 0 \tag{66}$$

With w and F determined it is now a simple matter to obtain all of the stress resultants and stresses. As far as pavement design is concerned, the critical stress is the radial tensile stress, σ_r, since asphalt is very weak in tension. Substituting Eqs. (49), (50), and (65) into Eq. (18) yields the general expression for σ_r in the form

$$\sigma_r = \frac{E}{(1-\nu)} \left[\frac{P}{B(1+\nu)} - \alpha T \right] \tag{67}$$

It is seen from Eq. (67) that the radial stress depends on the values of the coefficients of thermal expansion of the layers, the moduli of elasticity of the layers, Poisson's ratio, the thicknesses of the layers, and the character of the temperature distribution. The effect that each of these parameters has on the value of σ_r will now be investigated.

a) Coefficient of thermal expansion, α_i

The coefficient of thermal expansion will depend on the makeup of the asphalt layer. For this study, α_i will be taken to vary[2] from 1×10^{-5} to 1.4×10^{-5} in/in/°F.

b) Modulus of Elasticity, E_i

The modulus of elasticity of asphaltic concrete depends on temperature, and measured data relating E to temperature is available. In general, this relationship is nonlinear,[3,4] although a linear approximation is in some cases quite adequate over small temperature ranges.

In this report both linear and parabolic E-T relations are investigated.

c) Poisson's Ratio

In theory, the value of Poisson's ratio may vary from 0 to 1/2. For asphaltic concrete, the practical range appears to be from 0.3-0.5. However, the entire range is investigated.

d) The thickness of the layers

Although computer results have been obtained for a total thickness of up to twenty inches, this report is limited to a total depth pavement of six inches. Five specific cases are considered:

1) $t_1 = 1''$ $t_2 = 5''$?
2) $t_1 = 2''$ $t_2 = 4''$
3) $t_1 = 3''$ $t_2 = 3''$
4) $t_1 = 4''$ $t_2 = 2''$
5) $t_1 = 5''$ $t_2 = 1''$

It is felt that these combinations adequately illustrate the effect of relative layer thickness or stress levels in the pavement.

e) Character of the Temperature Distribution

The theory presented in this report is applicable only when the temperature in the pavement is low enough such that the time dependent (viscoelastic) part of the constitutive relations can be ignored. For this reason, the maximum temperature considered is approximately 60° F.

During the winter months of the year, the pavement temperature may vary[2] from about 0° F to 55° F. It is during this time of the year, when the pavement is brittle, that it is most susceptible to temperature gradient induced cracking. In the summer months, the viscoelastic properties of the pavement material provides for stress relaxation so that thermal stresses are not as critical. (The viscoelastic behavior of asphaltic concrete at high temperatures, although helpful when considering thermal stresses, unfortunately causes other serious problems.)

It has been shown[2] that the variation of temperature with depth in asphaltic concrete in the winter months may be approximated by a linear relation. Two different cases will be considered. In the first case, the temperature distribution will increase with depth, simulating an early winter morning condition. In the second case, the temperature will decrease with depth, as would occur in the early afternoon during a sunny day in winter.

Presentation of Results

The first series of graphs (Figs. 2-5) correspond to the case when Young's modulus is taken as a linear function of temperature in the form

$$E_i = a_i T + b_i \tag{68}$$

in which a_i and b_i are constants which may be different in each layer.

Since

$$T = cz + d \tag{69}$$

in which c and d are constants and z is measured from the top of the plate, Eq. (68) may be written as

$$E_i = e_i z + F_i \tag{70}$$

in which

$$e_i = ca_i \tag{71}$$

and

$$F_i = da_i + b_i \tag{72}$$

The two extreme temperature fields expressed in degrees Fahrenheit to be employed are

$$T_1 = 2.5z + 10 \tag{73}$$

$$T_2 = -3.5z + 53.3 \tag{74}$$

For each pavement considered, both temperature distributions were applied to the system. The maximum radial stress, σ_r, caused at some point in the plate by one of the temperature distributions is plotted in Figs. (2-8).

In Figs. (2-5),

$$a_1 = a_2 = -1.25 \times 10^5 \tag{75}$$

$$b_1 = 7.5 \times 10^6 \tag{76}$$

$$b_2 = 8.5 \times 10^6 \tag{77}$$

Figure (2) plots the variation of maximum radial tensile stress, σ_r, with Poisson's ratio. In this figure, both coefficients of thermal expansion were taken as 1.1×10^{-5}. For this case, the values of radial stress were largely independent of individual thicknesses of the plate layers. Therefore, only one average curve was drawn instead of five curves. Note the rapid increase in maximum radial tensile stress as Poisson's ratio increases. In fact, for $\nu = 0.5$, a very high and probably unsafe value of 1000 psi is present.

In Fig. (3), the maximum tensile stress is again plotted against Poisson's ratio but with different values of thermal expansion coefficients

in the two layers. As one would expect, the thicknesses of the individual layers now become very critical. The trend of increasing stress with increasing ν is still present, but the stresses can vary by as much as 27% depending on t_1 and t_2.

The maximum tensile stress is plotted against the coefficient of thermal expansion of the bottom layer in Fig. (4). In Fig. (4), $\alpha_1 = 1.1 \times 10^{-5}$ and $\nu = 0.35$. Note that when $\alpha_2 \tilde{=} \alpha_1$, the individual values of t_1 and t_2 are immaterial. As α_2 becomes larger than α_1, the maximum tensile stress increases. The worst case occurs when $t_1 = 1"$ and $t_2 = 5"$.

In Fig. (5), α_2 is kept constant and α_1 is varied. Once again, when $\alpha_1 = \alpha_2$, the thicknesses of the individual layers are not important. For $\alpha_1 > \alpha_2$, the variation of maximum tensile stress is more interesting than in Fig. (4). For certain thickness combinations, σ_r decreases for a time with increasing α_1 before increasing. Note the large difference in stress between the two extreme thickness cases when $\alpha_1 = 1.4 \times 10^{-5}$.

In the second series of graphs (Figs. 6-8), Young's modulus is taken as a parabolic function of temperature in the form

$$E_i = g_i T^2 + h_i T + k_i \tag{78}$$

in which g_i, h_i, and k_i are constants which may be different in each layer. In view of Eq. (69),

$$E_i = l_i z^2 + m_i z + n_i \tag{79}$$

in which

$$l_i = c^2 g_i \tag{80}$$

$$m_i = c(2dg_i + h_i) \tag{81}$$

$$n_i = d^2 g_i + dh_i + k_i \tag{82}$$

In Figs. (6-8),

$$g_1 = -74.1 \qquad h_1 = 148.2 \qquad k_1 = 1.657 \times 10^6 \tag{83}$$

$$g_2 = -92.5 \qquad h_2 = 185.17 \qquad k_2 = 2.07 \times 10^6 \tag{84}$$

Figure (6) plots maximum tensile stress vs. Poisson's ratio. The curves behave in a similar manner as those shown in Fig. (3) for the linear E-T relationship. The more complicated parabolic E-T expression, therefore, has little effect on the general trend of increased stress with increased ν.

In Fig. (7), α_2 is varied for the parabolic case. A comparison of Figs. (7) and (4) shows a marked contrast in behavior depending on whether the E-T relation is assumed to be linear or parabolic. In the parabolic case, stress levels decrease for a time with increasing α_2 except for the case when t_1 is one inch.

The coefficient of thermal expansion of the top layer is plotted against σ_r in Fig. (8). This graph also behaves quite differently from the corresponding linear case shown in Fig. (5). In Fig. (8), the stress levels increase almost linearly with increase in α_1. Note that in both Figs. (7) and (8), when $\alpha_1 \cong \alpha_2$, the maximum tensile stress is independent of the values of the individual thicknesses of the layers.

Work in Progress

Based on the results of the two layered system, the three layered case will only employ the more accurate parabolic relationship between temperature and Young's modulus. The results used in conjunction with the two layered case described herein will illustrate the effect and importance of a third layer in asphaltic concrete pavement design.

References

1. Timoshenko, S. and Woinowsky-Krieger, S., Theory of Plates and Shells, McGraw-Hill Book Co., Inc., New York, New York, 1959.

2. Finn, Frederick N., "Factors Involved in the Design of Asphaltic Pavement Surfaces", National Cooperative Highway Research Program, Report 39, Highway Research Board, 1967.

3. Van Der Poel, C., "Time and Temperature Effects on the Deformation of Asphaltic Bitumens and Bitumen-Mineral Mixtures", SPE Journal, September, 1955, pp. 47-53.

4. Southgate, Herbert F. and Dun, Robert C., "Temperature Distribution Within Asphalt Pavements and its Relationship to Pavement Deflection", Highway Research Board No. 291, Highway Research Board, 1969, pp. 116-131.

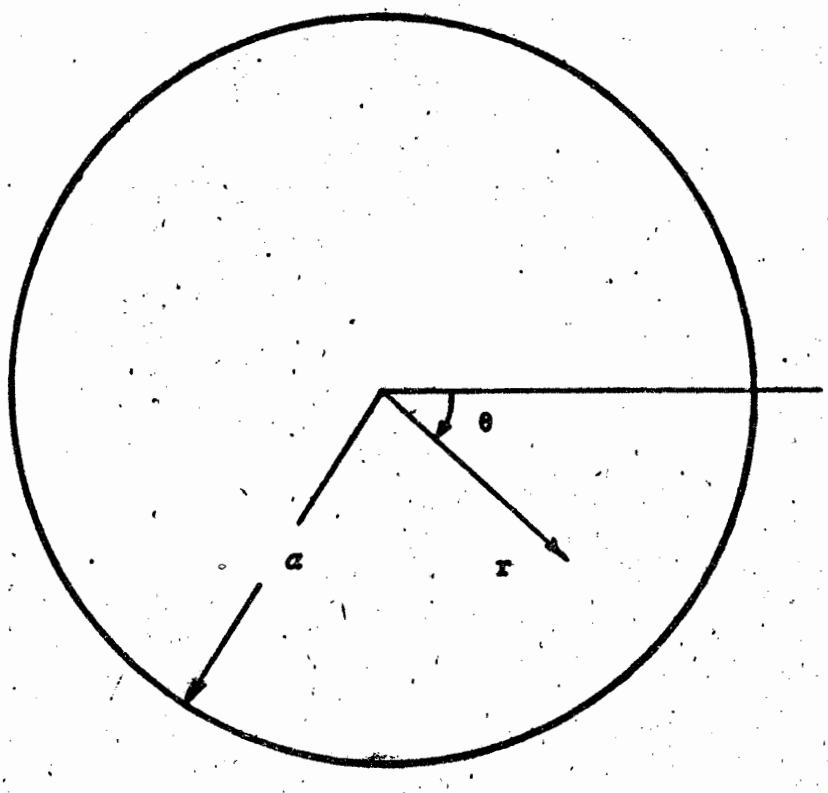

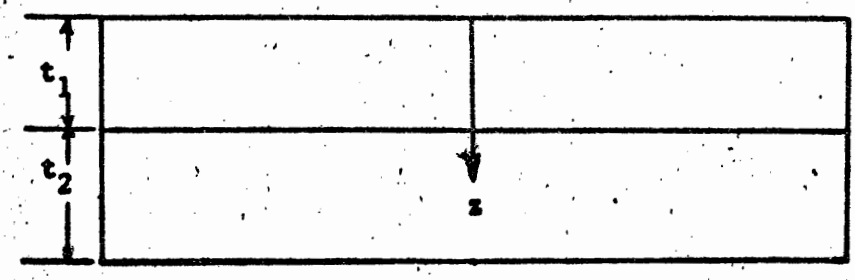

Fig. 1 - Laminated Plate

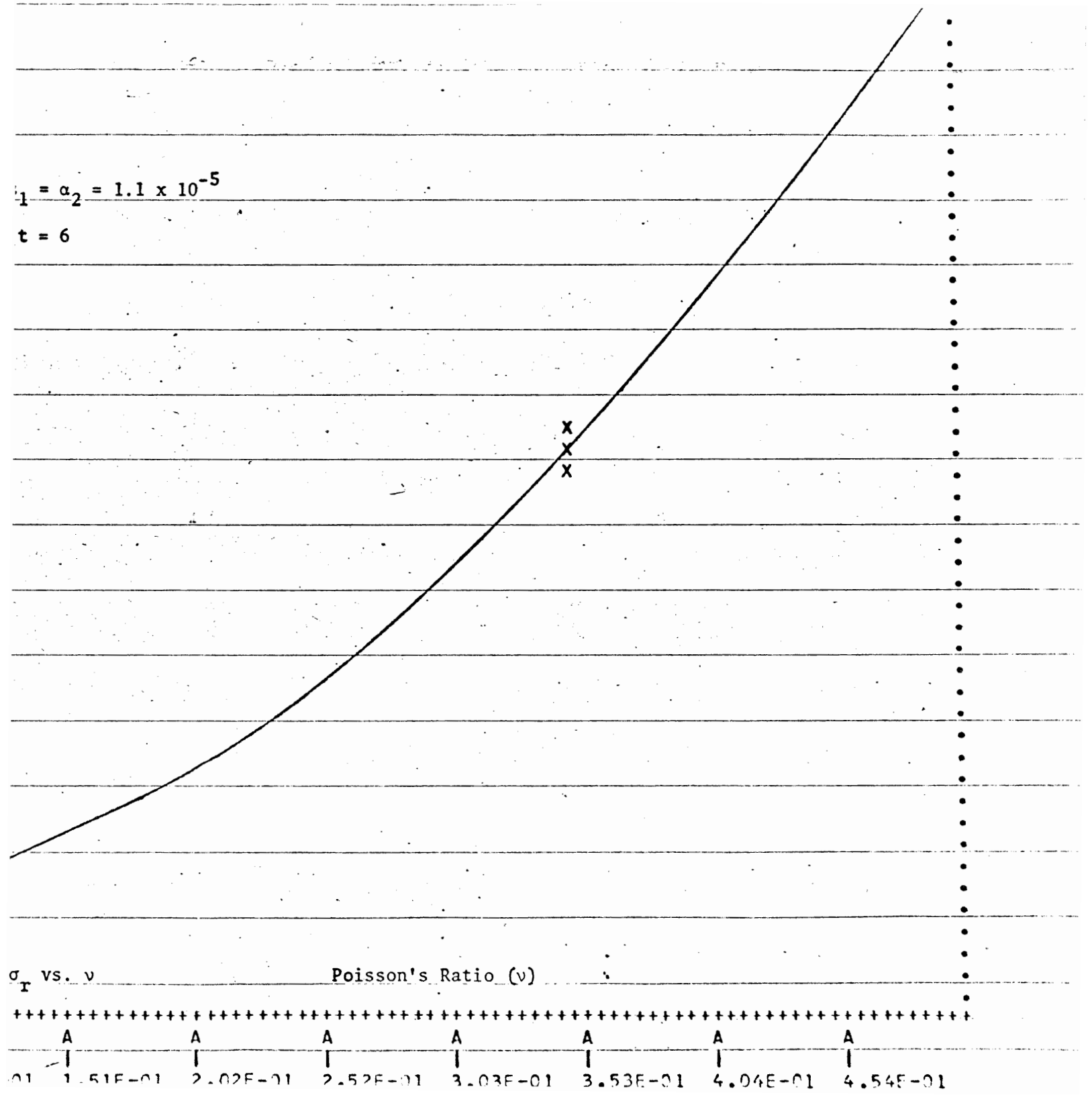
$\alpha_1 = \alpha_2 = 1.1 \times 10^{-5}$
t = 6
σ_r vs. ν
Poisson's Ratio (ν)
1.51E-01
2.02E-01
2.52E-01
3.03E-01
3.53E-01
4.04E-01
4.54E-01

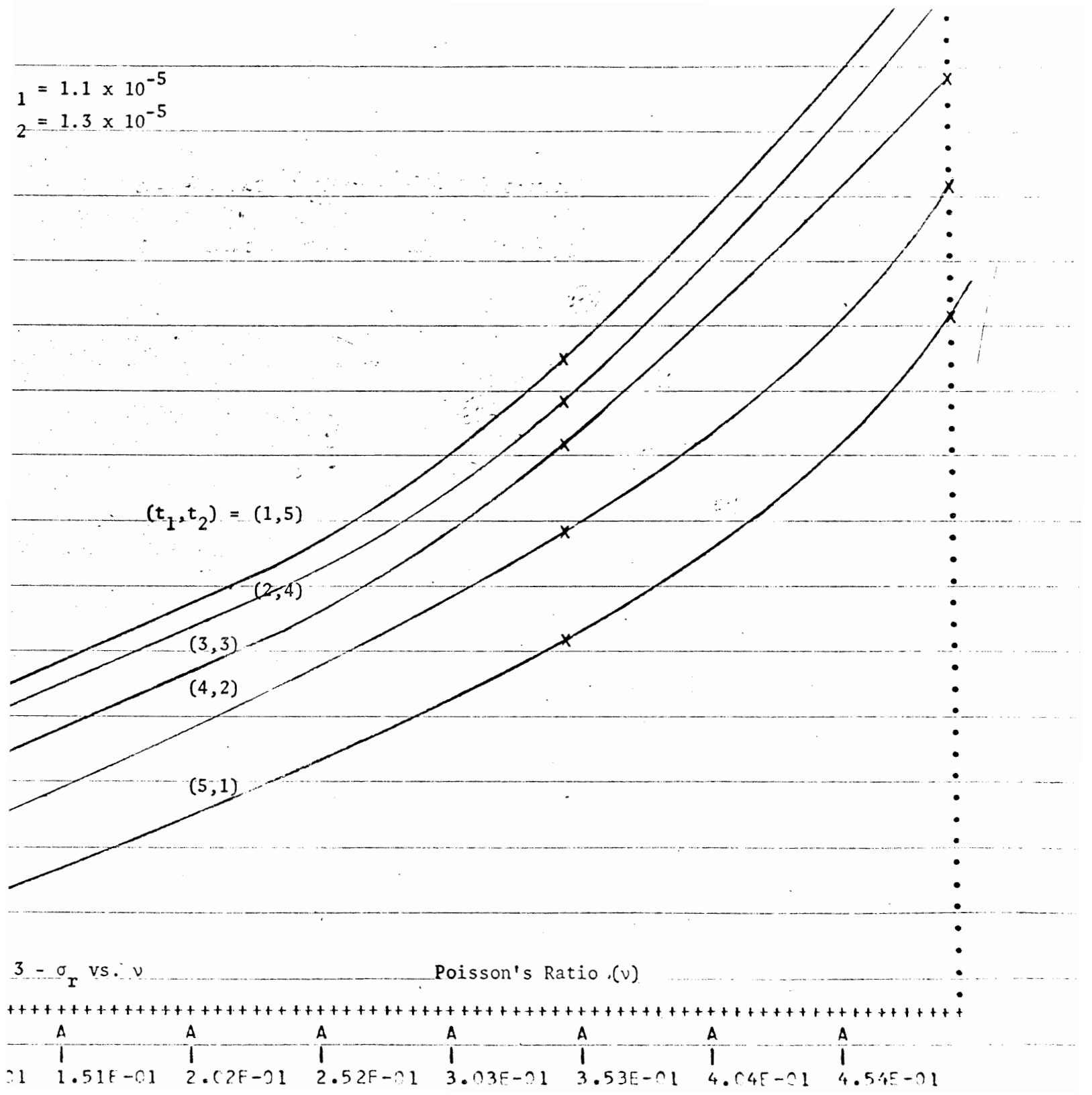
$_1 = 1.1 \times 10^{-5}$
$_2 = 1.3 \times 10^{-5}$
$(t_1, t_2) = (1,5)$
(2,4)
(3,3)
(4,2)
(5,1)
3 - σ_r vs. ν
Poisson's Ratio (ν)
01 1.51E-01 2.02E-01 2.52E-01 3.03E-01 3.53E-01 4.04E-01 4.54E-01

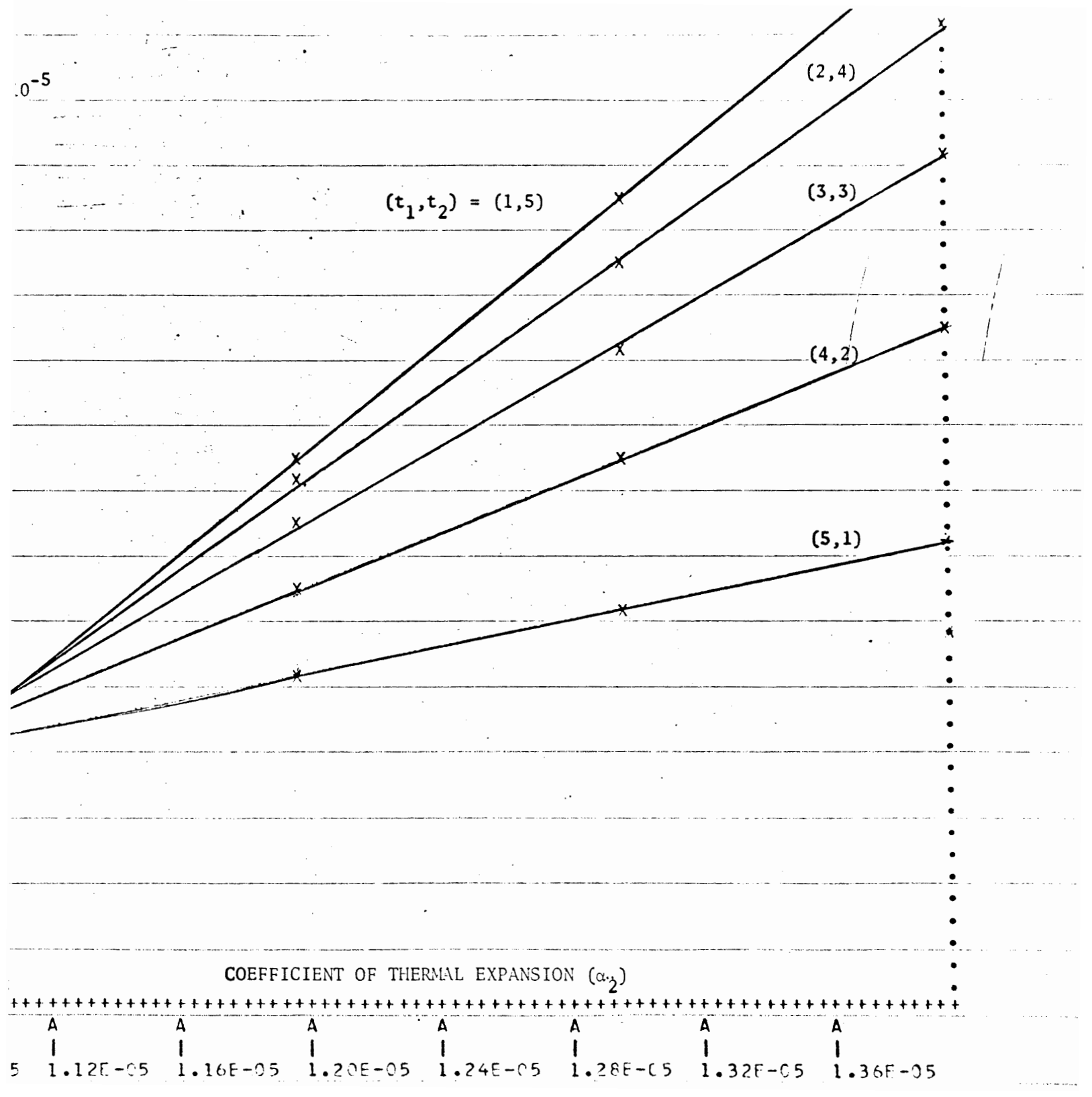
.0-5
(2,4)
(t1,t2) = (1,5)
(3,3)
(4,2)
(5,1)
COEFFICIENT OF THERMAL EXPANSION (α2)
5 1.12E-05 1.16E-05 1.20E-05 1.24E-05 1.28E-05 1.32E-05 1.36E-05

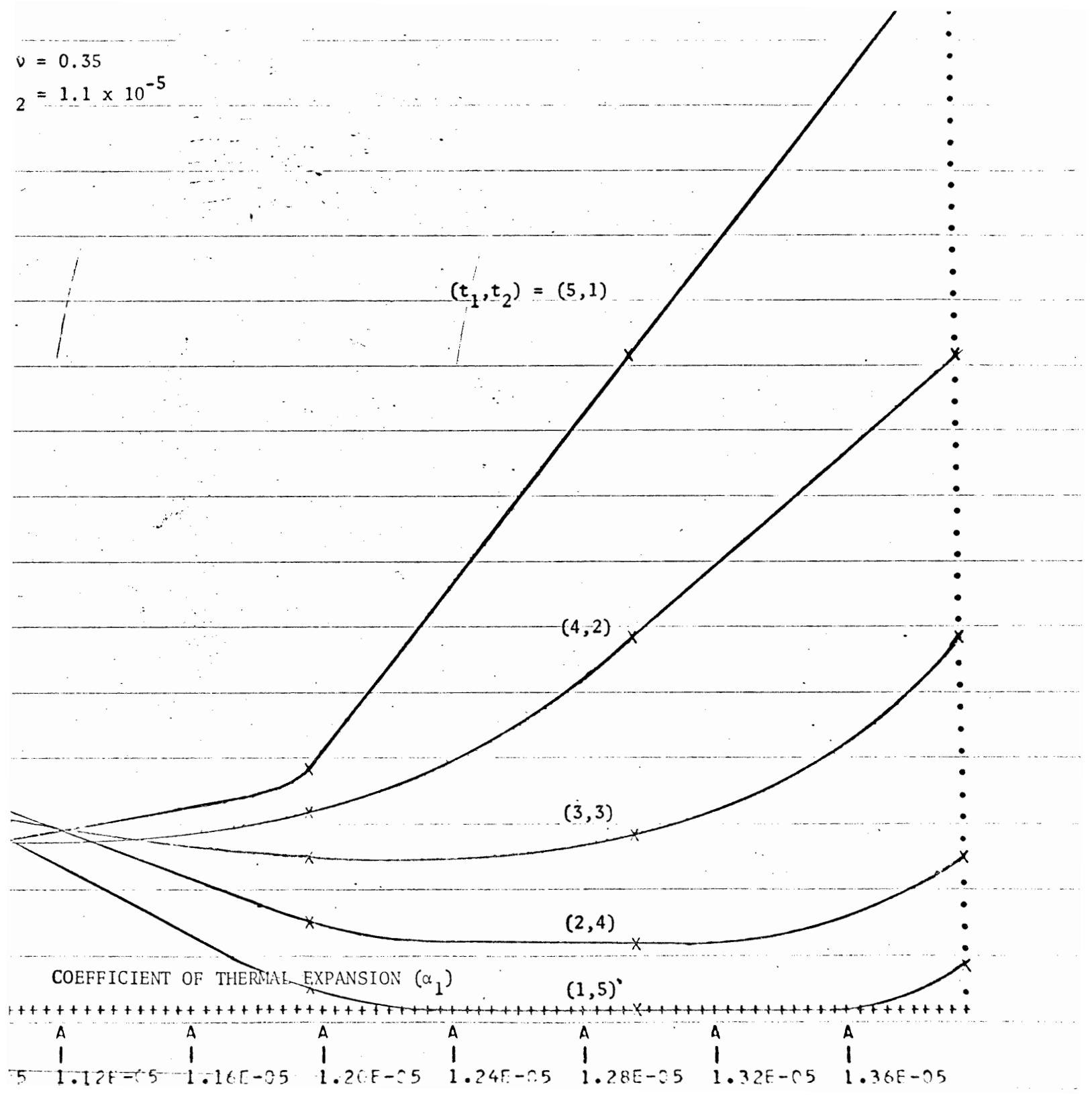
ν = 0.35
$\alpha_2 = 1.1 \times 10^{-5}$
$(t_1,t_2) = (5,1)$
(4,2)
(3,3)
(2,4)
(1,5)
COEFFICIENT OF THERMAL EXPANSION (α_1)
1.12E-05
1.16E-05
1.20E-05
1.24E-05
1.28E-05
1.32E-05
1.36E-05

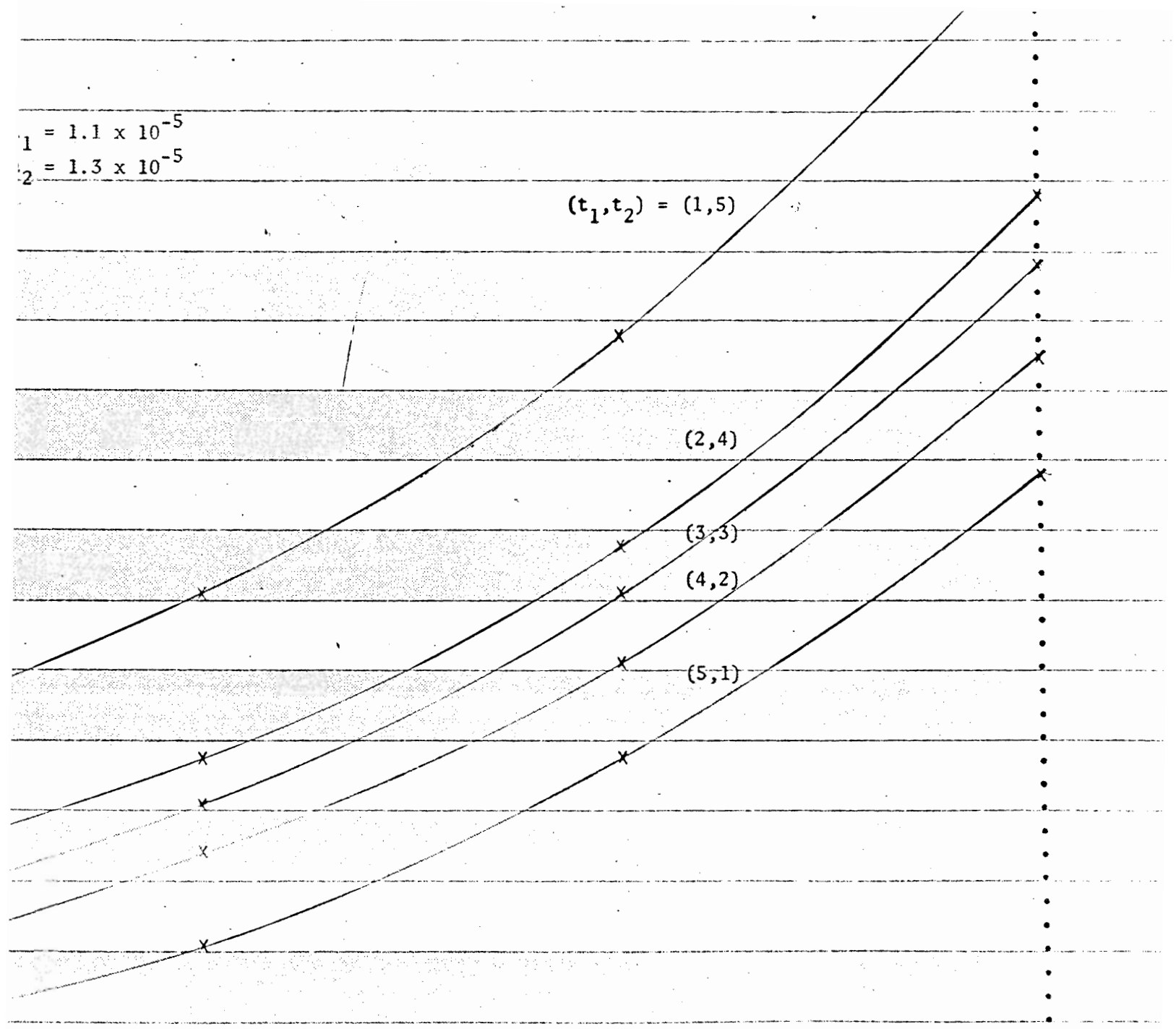

Fig. 6 - σ_r vs. ν Poisson's Ratio (ν)

-0.1 1.51E-01 2.02E-01 2.52E-01 3.03E-01 3.53E-01 4.04E-01 4.54E-01

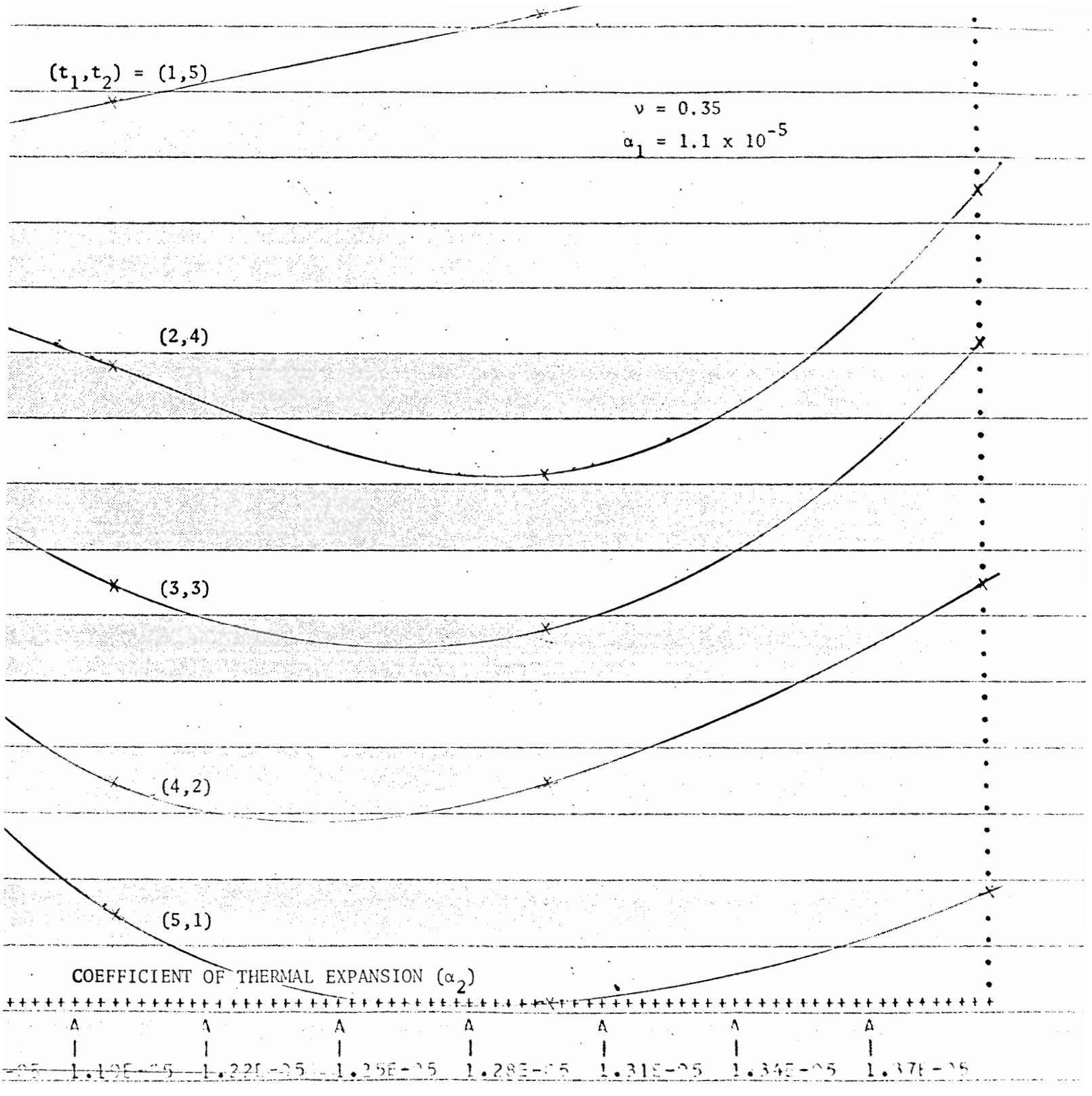
$(t_1,t_2) = (1,5)$
$\nu = 0.35$
$\alpha_1 = 1.1 \times 10^{-5}$
(2,4)
(3,3)
(4,2)
(5,1)
COEFFICIENT OF THERMAL EXPANSION (α_2)
1.19E-05
1.22E-05
1.25E-05
1.28E-05
1.31E-05
1.34E-05
1.37E-05

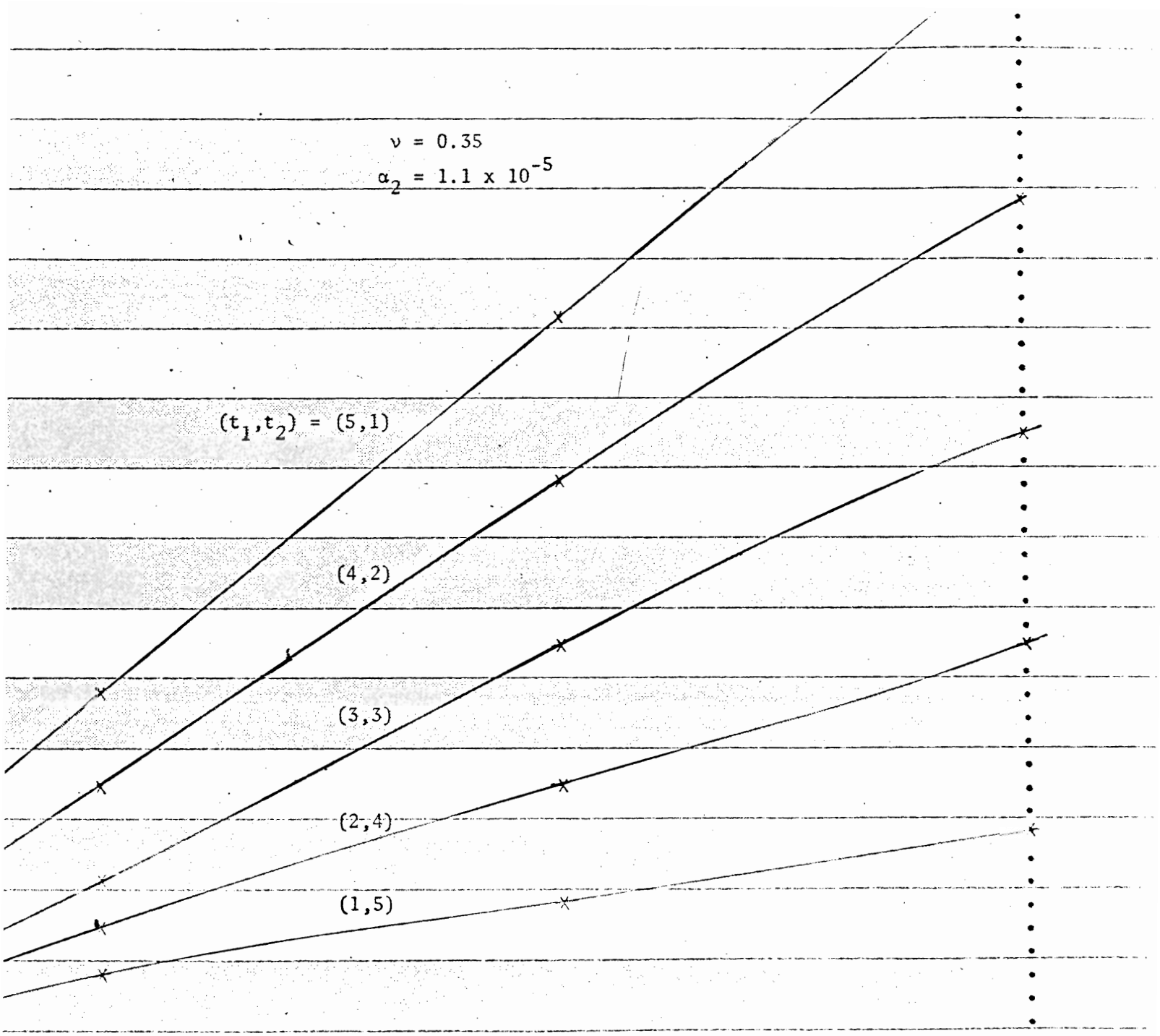

COEFFICIENT OF THERMAL EXPANSION (α_1)

Fig. 8 - σ_r vs. α_1

A A A A A A A

.25 1.19E-05 1.22E-05 1.25E-05 1.28E-05 1.31E-05 1.34E-05 1.37E-05